Resources for Quantum Information Processing

PROGRAM MANAGER

Prof Howard Wiseman – GU

MEASUREMENT AND CONTROL RESEARCHERS

Students Mr Joshua Combes (PhD), Mr Steve Jones (PhD), Mr Andy Chia (PhD), Mr Graham White (MSc)
Staff Prof David Pegg, Dr Joan Vaccaro, Dr Andrew Scott, Dr He-Bi Sun, Dr Austin Lund

COLLABORATING CENTRE RESEARCHERS

Griffith University, Australia
A/Prof Geoff Pryde
University of Queensland, Australia
Prof Gerard Milburn, Prof Tim Ralph
UNSW@ADFA, Australia
A/Prof Elanor Huntington
Macquarie University, Australia
Dr Dominic Berry

OTHER COLLABORATORS

Griffith University, Australia
Dr Eric Cavalcanti
Swinburne University, Australia
Dr Margaret Reid
University of Strathclyde, UK
Prof Stephen Barnett
Imperial College London, UK
Dr Sean Barrett
University College London, UK
Dr Ahsan Nazir
Perimeter Institute, Canada
Dr Robert Spekkens
University of Calgary, Canada
Dr Aidan Roy
University of Massachusetts, USA
Dr Kurt Jacobs
Stanford University, USA
Prof Hideo Mabuchi
University of Auckland, New Zealand
Prof Howard Carmichael
University of Tokyo, Japan
Prof Akira Furusawa

PROGRAM DESCRIPTION

The aim of this program is to further our knowledge of the resources necessary for quantum information processing, including quantum **measurement**, quantum **control**, and **entanglement**, to apply this knowledge to practical QIP as well as exploring its more **fundamental aspects**.

1. Quantum Measurement

The Hong-Ou-Mandel dip is a key diagnostic of the quality of single photons from solid-state single-photon sources. We studied the effects of realistic dephasing environments on this phenomenon [Nazir and Barrett, Phys. Rev. A **79**, 011804 (Rapid Comm.) (2009)]. By means of solutions for the Markovian or exact non-Markovian dephasing dynamics of the sources, we showed that the resulting loss of visibility depends crucially on the timing of photon detection events. Our results demonstrate that the effective visibility can be improved via temporal post-selection, and also that time-resolved interference can be a useful probe of the interaction between the emitter and its host environment.

We have also extended previous work on modelling continuous measurement of a coupled-dot solid-state qubit by a detector by considering a qubit with a non-zero energy gap [Sun and Wiseman, J. Phys. C **21**, 125301 (2009)]. The detector consists of a readout dot coupled to source and drain leads, with a tunnel rate through the detector is conditioned by the occupation number of the nearer quantum dot of the qubit and therefore probes the states of the qubit.
We gave a quantum trajectory analysis of the states of the coupled-dot device (qubit), and found quite different behaviour in the stochastic dynamics of the system from the degenerate case.

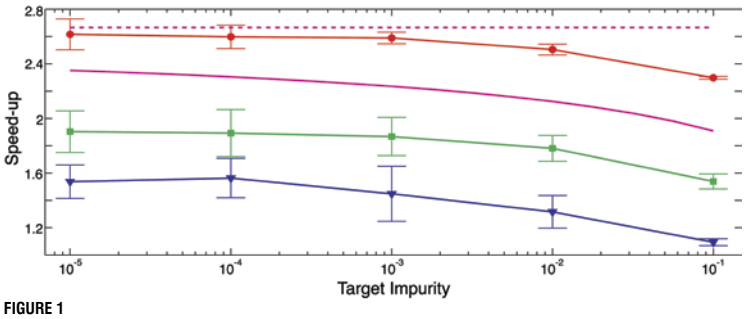

FIGURE 1

The purification speed-up provided by the random unitary strategy for $D = 4$. The solid curve is a lower bound on the speed-up in the limit where the time δt between unitary controls goes to zero, and the dashed line is its asymptotic (high-purity) limit. The circles, squares and triangles are numerical calculations of the speed-up with finite $\delta t = 0.01$, 0.25 and 1 (in units of the reciprocal measurement rate) respectively.

2. Quantum Control

We have continued to investigate control of quantum systems for rapid state purification (for preparation) and rapid read-out. Previously [Combes and Jacobs, Phys. Rev. Lett. **96**, 010504 (2006)] we had considered continuous measurement of the z-spin of a $D=2j+1$ dimensional system, and developed a feedback control algorithm giving an increase in average purification rate of order D. More recently we had developed a feedback control algorithm giving a decrease in the average time taken to read-out the state scaling as D^2 [Combes, Wiseman and Jacobs, Phys. Rev. Lett. **100**, 160503 (2008)]. This year we showed that both of these scalings can be obtained using continuous measurement and control without feedback [Combes, Wiseman, and Scott, to be published in Phys. Rev. A. (Rapid Comm.)] Specifically, we considered random controls, drawn from the unitary group in the first case and the permutation group in the second. A non-feedback control strategy has the great advantage of avoiding delays in the feedback loop, which adversely affect performance. We showed that the protocols work well for controls applied at periodic times, especially for the purification problem where the frequency can be of order the measurement rate.

In the area of adaptive measurements, we have followed up our work on generalizing the quantum phase estimation algorithm (QPEA) [Higgins, Berry, Bartlett, Wiseman, and Pryde, Nature **450**, 393–6 (2007)] by publishing the theoretical foundations for it, with further analytical and numerical results [Berry, Higgins, Bartlett, Mitchell, Wiseman, and Pryde, Phys. Rev. A. **80**, 052114 (2009).] First, we derived the Heisenberg limit to the accuracy of interferometric phase measurement in complete detail for the first time, in terms of N, the number of fringes per wavelengths summed over all instances of fringe-numbers employed. Next, we showed that arbitrary inputs to an interferometer can be analysed in terms of equivalent two-mode states, and we showed numerically and analytically that for our generalized QPEA, the input states have an intrinsic phase variance scaling as the Heisenberg limit as long as M is 3 or greater. Here the fringe numbers are restricted to powers of two, and M is the number of times each such fringe-number is instantiated. Then we showed that the measured phase variance using our generalized QPEA is Heisenberg-limited as long as M is 4 or greater, with analytical results for the cases $M = 1$ and 2. Finally, we showed, analytically, numerically and experimentally, that increasing M while keeping the maximum fringe-number fixed does not give Heisenberg-limited precision, but rather precision scaling the same as the standard quantum limit. (This paper also contained work relating to other algorithms which is being reported to the ARC elsewhere.)

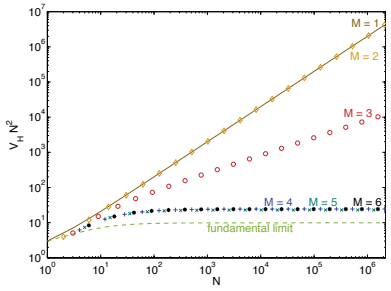

FIGURE 2

The phase variance multiplied by N^2 for M varying from 1 to 6. The results for M = 1 are shown as the solid line, for M = 2 as the diamonds, for M = 3 as the circles, for M = 4 as the pluses, for M = 5 as the crosses, and for M = 6 as the asterisks. The Heisenberg limit is also shown as the dashed line for comparison.

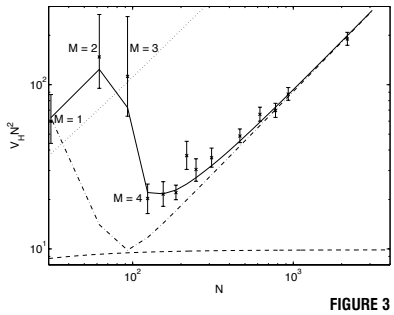

FIGURE 3

The theoretical predictions and experimental results for the phase variance multiplied by N^2 for a maximum fringe-number of 16 (achieved experimentally by multiple passes), and a range of values of M given by $M = N / 31$. The solid line is the predictions for the generalized QPEA, the dashed-dotted line is the intrinsic variance, and the crosses and error bars are for the experimental data. The SQL for single passes is shown as the dotted line, and the dashed line is the Heisenberg limit.

3. Entanglement

We have continued to investigate the concept of steering, introduced by Schrödinger as a generalization of the Einstein-Podolsky-Rosen (EPR) paradox but only recently formalized by us [Wiseman, Jones, and Doherty, Phys. Rev. Lett. **98**, 140402 (2007)]. We have now developed a general theory of experimental EPR-steering criteria [Cavalcanti, Jones, Wiseman and Reid, Phys. Rev. A **80**, 032112 (2009)]. We derived a number of criteria applicable to discrete as well as continuous-variable observables, and studied their efficacy in detecting this form of nonlocality in some classes of quantum states. We showed that previous versions of EPR-type criteria can be rederived within this formalism, thus unifying these efforts from a modern quantum-information perspective and clarifying their conceptual and formal origin. The theory followed in close analogy with criteria for other forms of quantum nonlocality (Bell nonlocality and entanglement).

4. Fundamental aspects of QIP

Quantum teleportation is a primitive in quantum information processing, and has continuous-variable as well as qubit versions.

In a collaboration with University of Auckland researchers we investigated the quantum teleportation of the temporal fluctuations of light [Noh, Chia, Nha, Collett, Carmichael, Phys. Rev. Lett. **102**, 230501, (2009)]. We considered to what extent it is possible to teleport a beam of light such that the light beam that emerges at the teleporter output carries over all of the quantum statistical properties of the beam at the input. We focused our attention on photon correlations, specifically photon anti-bunching as produced by a driven atom with damping rate γ_i. As quantified by $g^2(0)$, this is a standard measure of quality of photon sources. We showed that for sufficiently good squeezing, of sufficiently broad bandwidth γ_s, and with optical filters of appropriate bandwidth γ_B, high-quality photon antibunching can be seen at the teleporter output.

The necessity of optical coherence for quantum teleportation has been a controversial issue, and we have addressed this question (and the origin of optical coherence in general) in a paper selected for a Viewpoint in the on-line APS journal "Physics" [Pegg, Phys. Rev. A **79**, 053837(2009)]. This work shows that any initial state of a single-mode cavity, provided it has a reasonably narrow photon-number distribution, will give rise to an output almost indistinguishable from that of a coherent source.

Finally, we have continued our work on unitary t-designs [Roy and Scott, Designs, Codes and Cryptography **53**, 13 (2009)]. A unitary t-design is a collection of unitary matrices that approximate the entire unitary group. They have applications in quantum information theory, for defining optimal measurements for quantum process tomography and to provide a means to derandomize certain quantum information processing tasks that would otherwise require random unitaries (which cannot be implemented efficiently on a quantum computer). We used irreducible representations of the unitary group to find a general lower bound on the size of a unitary t-design in U(d), for any d and t. We also gave an upper bound on the size of the smallest weighted unitary t-design in U(d), and catalogued some t-designs that arise from finite groups.

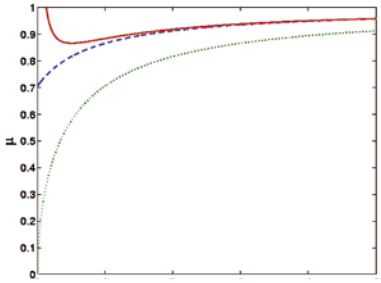

FIGURE 4

Boundaries between different classes of symmetric two-mode Gaussian states parameterized by mean one-sided photon number n and a purity measure μ. The lower line (green, dotted) is the entanglement boundary: all and only states above the line are entangled. The central (blue, dashed) line is a steerability lower boundary based on the Reid multiplicative variance criterion for the EPR paradox: all states above this line are steerable. The upper line (red, full) is another steerability lower boundary based on a generalization of the additive variance entanglement criterion of Duan *et al* and Simon: states above this line are steerable.

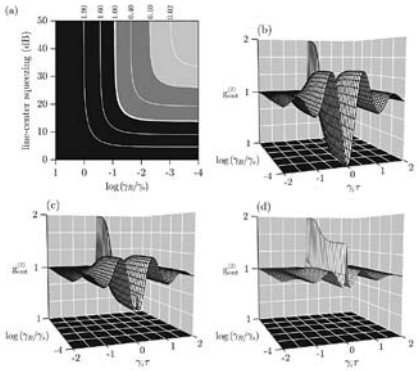

FIGURE 5

Teleportation of photon antibunching: (a) contours of $g^2(0)$ at the teleporter output. In the remaining plots $g^2(\tau)$ is shown for different degrees of squeezing at line-centre: (b) 45 dB; (c) 15 dB; and (d) 10 dB. The strength of the atomic driving (Rabi frequency) is $\Omega = 6\,\gamma$.